X-Ray Measurements of the Mass Distribution in the Dense Primary Break-Up Region of the Spray from a Standard Multi-Hole Common-Rail Diesel Injection System

P. Leick*[1a], T. Riedel[1b], G. Bittlinger[1a]
C.F. Powell[2a], A.L. Kastengren[2a], J. Wang[2b]
[1a] Robert Bosch GmbH, Corporate Research, Gerlingen, Germany
[1b] Robert Bosch GmbH, Diesel Systems, Stuttgart, Germany
[2a] Center for Transportation Research, Argonne National Laboratory, Argonne, IL, USA
[2b] Advanced Photon Source, Argonne National Laboratory, Argonne, IL, USA

Abstract
Unlike most quantitative optical measurement techniques, x-ray-radiography is not restricted by multiple scattering effects, and it has been demonstrated in recent years that the mass distribution in a Diesel spray can be deduced from the measured extinction of a monochromatic x-ray beam, even in the dense near-nozzle region. In prior applications of the technique, single-orifice research nozzles were used to inject the fuel in atmospheres of lower density or pressure than at typical engine conditions. The first application involving near-standard production nozzles and injections into atmospheres of representative densities is reported in this paper. The sprays are found to be rather symmetric and stable, with the bulk of the fuel mass concentrated in a narrow region around the nozzle axis.

Introduction

The injection system of a modern Diesel engine plays an important role on the fuel/air mixture preparation, hence on power, fuel consumption and emissions [1]. At the current high level of engine development, further improvements can only be based on a detailed understanding of all the processes involved in the atomization of the fuel jet and its subsequent evaporation and combustion. However, current models of the internal structure of high-pressure Diesel sprays are still tentative, reflecting the limited amount of available reliable experimental data [2]. Studies of fuel sprays typically rely on non-intrusive optical measurement techniques, but in the dense primary break-up region close to the nozzle outlet, the spray core is generally surrounded by a cloud of small droplets that is opaque to visible light. Information obtained from most optical measurement techniques is thus restricted to the spray periphery which, however, contains only a small fraction of the total fuel mass.

In the x-ray part of the electromagnetic spectrum, absorption replaces elastic scattering as the dominant interaction mechanism between fuel parcels and incoming photons. Since the attenuation of a monochromatic x-ray beam does not depend on the exact shape of the spray, but only on the total fuel mass contained within the beam path, x-ray radiography can be used to map the mass distribution in the spray, even in the dense near nozzle region. Several applications of this technique have been reported by Argonne National Laboratory (ANL) and collaborators, with spray characteristics such as local fuel density, droplet accumulation at the spray tip and different definitions of jet velocities being investigated [3-6].

In previous experiments, custom-made nozzles with a single axial hole were used. An extension of x-ray radiography to multi-hole production nozzles is not straightforward, as neighboring jets will obstruct the one being observed. The high ambient densities needed to simulate the conditions found in a Diesel combustion chamber at the moment of injection are an additional challenge, as pressurized atmospheres and thick chamber windows can absorb a significant percentage of the incoming x-rays. To date, studies on the effects of ambient density have thus been limited to densities well below the desired range [4, 5].

The significance of these restrictions should not be underestimated. It is generally recognized that the density of the surrounding gas is the ambient parameter with the highest influence on the propagation and the breakup of Diesel-type jets [7]. Fuel flows in single-hole-axial and multi-hole nozzles are fundamentally different, as the inflow towards the spray hole(s) should be symmetric in the first and asymmetric in the latter case, which has been shown to affect spray formation via higher turbulence levels and may also lead to asymmetric breakup and/or deviations between the nozzle axis and the main spray direction [8].

For the present measurement campaign, a compact pressure vessel was specially developed to meet the requirements of x-ray radiographies of Diesel sprays at high ambient densities and to accommodate multi-hole nozzles. To the knowledge of the authors, no other quantitative characterization of the dense near-nozzle region of a Diesel spray has been reported under conditions that can be considered closer to an actual Diesel environment.

* Corresponding author.
E-Mail: philippe.leick@de.bosch.com
Proceedings of the 21st ILASS - Europe Meeting 2007

Experimental Setup

The experiments described in this report were performed at the 1-BM beam line of the Advanced Photon Source (APS) at Argonne National Laboratory (ANL). The synchrotron radiation produced by the APS, a 7 GeV electron storage ring, first passes through a collimating mirror, then through a double crystal Bragg-Bragg monochromator. This creates a narrow x-ray beam with photon energies of E_ν and its integer multiples. Finally, a harmonic rejection mirror creates a narrow bandwidth ($\Delta E/E_\nu \approx 10^{-4}$) beam with a size of about 1×1 mm^2 and directs it towards the experiment (Fig. 1).

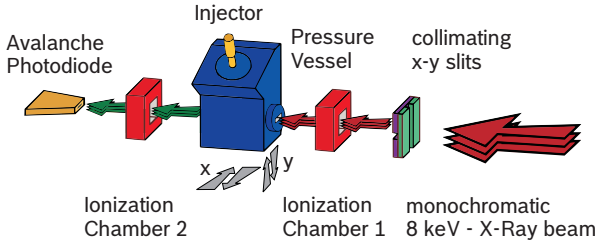

Figure 1: schematic representation of the experimental setup. The pressure vessel is mounted on a computer-controlled *x*-*y*-translation stage.

Spatial resolution is limited by the size of the beam at the spray location. Therefore, before entering a pressure vessel with specially designed thin x-ray windows, the beam size is reduced to about 167 µm (FWHM, full width half maximum) in axial (x) and 29 µm FWHM in transverse (y) direction using a pair of vertical and horizontal slits. The energy of each x-ray pulse passing the spray chamber is measured by an Avalanche Photodiode (APD) and recorded with a digitizing oscilloscope. As a control, the time averaged beam power is continuously monitored by two ionization chambers.

The fuel is injected into the pressure vessel using a Bosch common rail (CR) injector and fuel supply system capable of delivering rail pressures up to p_I = 135 MPa. A standard 6-hole production nozzle (Table 1) is mounted to the injector. 3 of the 6 orifices were closed in order to minimize the amount of fuel droplets deposited on the chamber windows. It is important to note that the fuel flow from the needle seat towards the spray holes remains symmetric around the injector axis despite the reduced number of orifices. The symmetry of the three remaining jets was verified in an optically accessible spray chamber [9] during the preparation of the x-ray radiographies.

Nozzle type	Orifice geometry	Outlet diameter	Height angle
VCO	ks 1.5	D_O = 145 µm	Ψ = 80°

Table 1: relevant nozzle properties [10]

For the investigations presented here, 12.5 mm^3 of fuel were injected at a rail pressure of p_I = 80 MPa, corresponding to an injection duration of ~0.66 ms. The spray chamber can be pressurized up to $p_G \le 1.9$ MPa. When filled with nitrogen (N_2) at room temperature, the maximum pressure is equivalent to a gas density of ρ_G = 21.7 kg/m^3, a typical value at the moment of injection in a passenger car engine at high part-load-conditions. To study the effect of gas density on the spray properties, the experiments were repeated at a lower value of ρ_G = 11.4 kg/m^3 (p_G = 1.0 MPa). As the nozzle employed in this study is free of cavitation, changes in nozzle flow due to the decreased back pressure p_G are assumed to be negligible and all observed differences can be attributed entirely to the interaction of the liquid fuel with the surrounding atmosphere.

In order to increase the x-ray extinction coefficient of the fuel, it has to be doped with a cerium (Ce) additive. The x-ray absorption of materials is strongly dependent on photon energy, which is thus selected in order to maximize the absorption of fuel and additive compared to the extinction due to the chamber fill gas. However, even at the photon energy (E_ν = 8 keV) used in this study, the nitrogen is responsible for a significant part of the observed x-ray extinction.

Data Processing

For monochromatic x-rays, the beam attenuation is described by the simple Lambert-Beer-law:

$$I(t) = I_0 \exp\left[-\int \mu_M \rho(z,t)\,dz\right] = I_0 \exp\left[-\mu_M \cdot M'(t)\right]. \quad (1)$$

In this equation, $I(t)$ and I_0 are the transmitted and incident beam intensities (i.e. during and before the injection), μ_M is the extinction coefficient (per mass/area) and ρ the *local* fuel density in the spray, which will generally be lower than the density of undisturbed liquid. $M' = \int \rho(z)\,dz$ is the projected mass per unit area along the beam path. With the assumption that I_0 is constant during the injection, it is straightforward to calculate $M'(t)$ at different positions in the spray using Eq. 1.

It should be stressed here that since radiography is a line-of-sight technique, the measured data points M' represent the projection of the actual, three-dimensional mass distribution on a two-dimensional plane perpendicular to the x-ray beam. Accordingly, M' is measured in units of mass/area [µg/mm^2].

During each injection, the attenuation is measured only for the small portion of the spray illuminated by the x-ray beam (coordinates: x, y). The spatial spray structure is examined by moving the spray chamber to many different positions along an optimized irregular measurement grid, performing measurements at each point. Furthermore, the signal-to-noise ratio is improved by averaging the attenuation traces for 64 different injections. Since two-dimensional representations of the spray structure (see Fig. 2) need to be based on a regular grid of data points, a Renka-Cline interpolation algo-

rithm [11] is used to calculate values at closely spaced regular locations in the spray.

Further analysis may be based on the $M'(t)$ data sampled along this regular grid. In a first step, for any given time moment t, the center of mass is calculated at each distance x from the nozzle outlet (δy_i being the radial distance between successive measurement positions):

$$y_0(x,t) = \frac{\sum_i y_i \cdot M'_i(x,y_i,t) \cdot \delta y_i}{\sum_i M'_i(x,y_i,t) \cdot \delta y_i} \qquad (2)$$

Fitting this data to a straight line yields the position and orientation of the spray axis, which is then used to derive additional information such as the penetration of the spray tip or the projected mass along the spray axis.

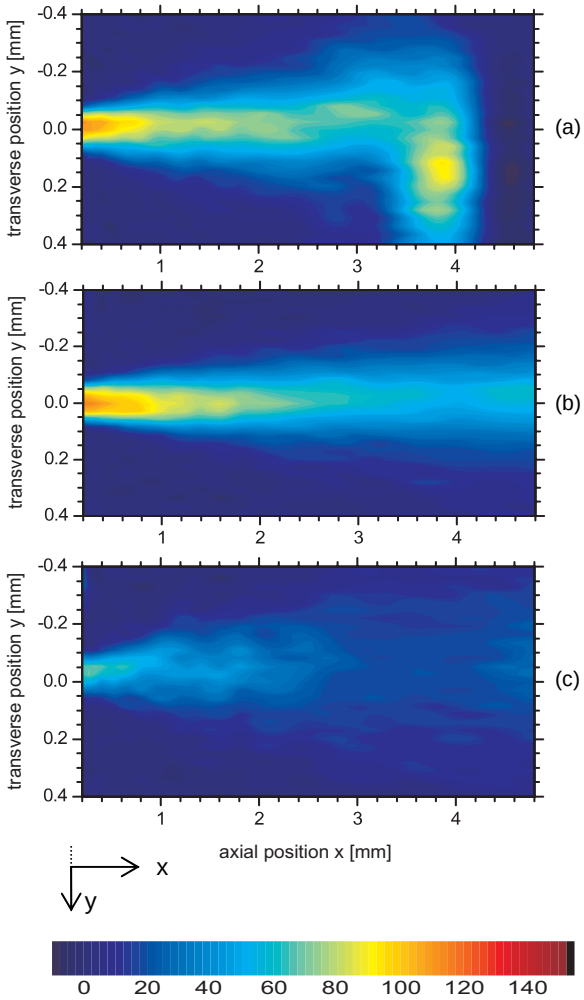

Figure 2: Projected mass/area [µg/mm^2] at the beginning (a, t = 0.37 ms), during the quasi-steady-state phase of (b, t = 0.70 ms) and at the end (c, t = 1.02 ms) of the injection (ρ_G = 21.7 kg/m^3).

A direct evaluation of the width (FWHM) of the radial profiles $M'(y)$ would be extremely sensitive to noise. To overcome this difficulty, the data is fitted to a general peak function with 5 independent parameters (Fig. 3), which also yields the position of the maximum of $M'(y)$. The asymmetry of the radial profile can be defined based on a comparison of the total measured mass on either side of this position.

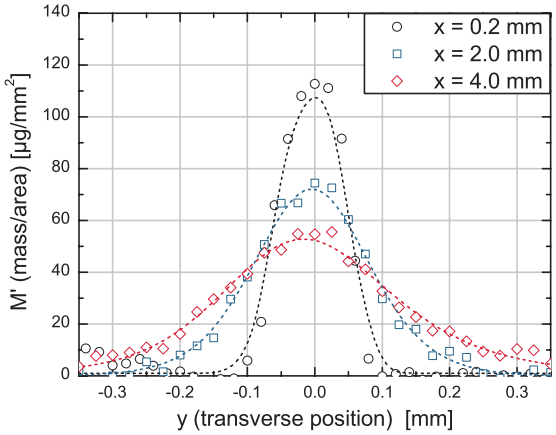

Figure 3: Transverse mass distributions $M'(y)$ for different distances x from the nozzle outlet (symbols) and corresponding fit (dotted lines).
t = 0.7 ms, ρ_G = 21.7 kg/m^3.

Mass Distribution in the Primary Breakup Zone

Some examples of projected fuel mass distributions during different phases of the injection are shown in Fig. 2. The time t is measured in relation to the start of energization of the solenoid coil. Liquid fuel starts exiting the nozzle about 340 µs later, and the injection stops near t = 1.0 ms.

Near the beginning of injection (Fig. 2a, while the complete spray is visible), the velocities of the spray's leading edge are lower at higher ambient gas densities, even though the spray is not yet fully developed. But apart from the spray tip region, the projected mass distributions at lower gas density are almost identical to those shown in Fig. 2.

The highest values of M' are found near the nozzle outlet and also in the leading edge of the spray, where mass accumulates as fast droplets catch up with droplets injected earlier at lower velocities and decelerated by the surrounding gas. The higher values of M' in the spray tip (Fig. 2a) are not necessarily due to a higher local density, but more probably to the widening of the spray tip. The typical mushroom shape of Diesel sprays (caused by accumulation processes that push fuel away from the spray axis) well known from optical investigations can be recognized in the projected mass distributions.

Especially during the quasi-steady state phase of the injection (Fig. 2b), where the needle lift is high enough not to restrict the fuel flow towards the spray holes, the fuel mass is concentrated in a very narrow zone around the nozzle axis. Careful examination of the projected mass distributions reveals that only a very small amount of mass is located at greater distances from the nozzle axis (compare with Fig. 3). At the end of injection

(Fig. 2c), the needle moves back towards its seat and the nozzle flow is throttled, which leads to increased turbulence. This in turn causes a significant widening of the spray cone. Just before the end of injection, the velocity of the fuel droplets leaving the orifice is very low and some of them can remain in the vicinity of the outlet for a long time, which explains the persistence of fuel near the orifice after the injector closes.

While the projected mass plots give a rapid overview of the spray structure, they are not ideally suited for a detailed analysis of important spray features, and color scales tend to highlight some specific values at the expense of others. Therefore, characteristic spray properties are identified and suitable methods for their calculation and evaluation suggested. In the following sections, some of these quantities will be presented and discussed.

Spray Direction and Cone Angle

The values of the spray axis direction and of the cone angle calculated from the x-ray-measurements are displayed in Figs. 4 and 5, respectively. For sharp-edged, cavitating nozzles, deviations of several degrees between nozzle and spray axes have been previously observed [8]. This is not the case here: the spray direction remains constant during the whole injection and the divergence between spray and nozzle axis is lower than 0.5°. The stability of the main spray direction is an important result, as the exact location of the impact point between fuel vapor and piston bowl can have a large influence on combustion and pollutant formation [13].

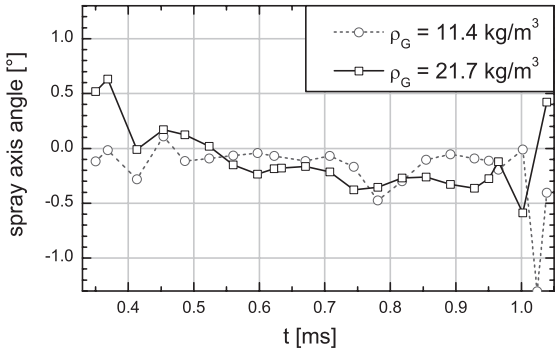

Figure 4: Deviation between spray and nozzle axis. The higher values at the beginning of injection (at $\rho_G = 21.7$ kg/m^3) are entirely due to the asymmetric mass distribution in the spray tip. Slightly higher deviations near the end of injection ($t > 1$ ms) involve only a negligible fraction of the total fuel mass.

The values of the cone angle (CA) shown in Fig. 5 illustrate the fact that gas density seems to have little influence on the mass distribution in the near-nozzle region. The lowest cone angles (~2.5°) are found at times when the needle lift is high ($t \sim 0.55$ - 0.95 ms). The high CA at the beginning of the injection is not entirely due to the passage of the wide spray tip, which leaves the measurement domain at $t \approx 0.38$ ms. During the early ($t \leq 0.5$ ms) and late ($t \geq 0.95$ ms) stages of the injection, the nozzle flow is less regular and the cone angles are much higher. This trend has been observed previously in optical spray investigations [14], but the mass distributions represent the spray dynamics more accurately.

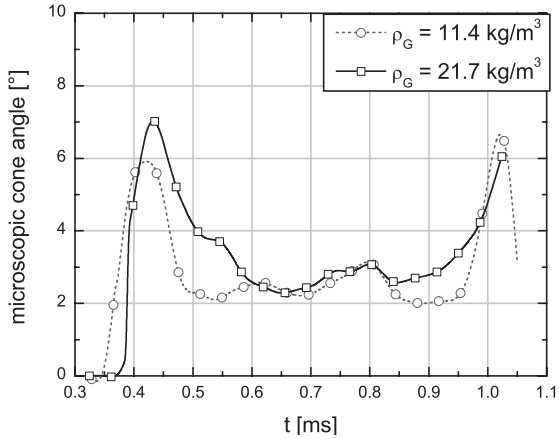

Figure 5: Spray cone angle as a function of time. The calculation is based on the difference of the spray widths (FWHM) at $x = 0.2$ and $x = 4.0$ mm.

The absolute values of the spray cone angles are much lower than corresponding values derived from optical measurement techniques which probe only the spray periphery (~ 12° for the conditions considered here, see Fig. 6). While the droplet concentration in the outer regions of the spray is high enough to be clearly visible, it is not so high as to contain a sizeable amount of the total spray mass. The differences in CA values based on optical and x-ray measurements are not in contradiction but simply reflect the fact that they are derived from different spray properties.

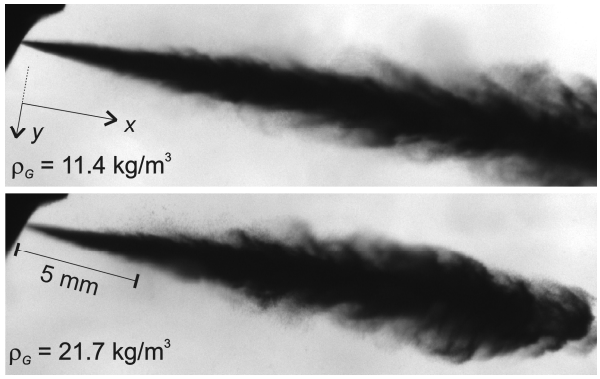

Figure 6: Shadowgraphs (24 × 7 mm) of the spray at $t = 0.55$ ms (quasi-steady-state phase). At higher gas density, the spray tip penetration is lower and the spray plume has a larger width than at low ρ_G, but the differences are only noticeable at distances from the nozzle exit higher than $x \sim 5$ mm. The optical microscopic cone angle ($0 \leq x \leq 5$ mm) is of the order of $CA_{Opt} \sim 12°$ and independent of ρ_G.

The results of our investigations complement earlier work [4-5], where it has been found that, in a lower range of gas densities (ρ_G = 1 - 6 kg/m^3), spray cone angles calculated from x-ray radiography measurements are lower than corresponding optical cone angles and do not increase with ρ_G.

It is interesting to compare the ρ_G-dependency of the width of the mass distribution with velocity profiles measured in the primary breakup region of Diesel sprays very similar to the ones investigated here [12]. A rise in ambient gas density had no significant effect on the high velocities near the spray axis. However, the width of the transition region in which the mean velocity decreases with increasing distance from the spray axis was actually *lower* at higher ρ_G, which was attributed to a more rapid deceleration of droplets outside of the dense spray core. Both at low and at high ρ_G, slow droplets with no clearly defined main flow direction could be detected beyond the transition region. Since the concentration of these droplets is low (compared to the spray center), they do not contribute significantly to the mass distributions. But they are readily visible using optical measurement techniques. We therefore suggest that such droplets account for the high spray widths typically deduced from optical experiments.

Mass distribution along the spray axis

Figure 7 shows the mass distribution along the fuel jet axis $M'(x, y_0)$ for two different times during the spray's evolution. Additionally, the total mass/length in planes orthogonal to the nozzle axis is calculated according to

$$M'_L(x) = \sum_i M'(x, y_i) \cdot \delta y_i \qquad (3)$$

and displayed in Fig. 7. At t = 0.37 ms, the spray tip is clearly visible in the projected mass plots (compare Fig 2a), while the later time of 0.7 ms corresponds to the quasi steady injection phase, during which the total mass/length at different distances from the nozzle outlet is nearly constant and the projected mass on the spray axis diminishes roughly as $(1+\alpha x)^{-1}$, as should be expected for a conical spray.

The mass accumulation at the spray tip can clearly be seen at t = 0.37 ms. Between the nozzle outlet and the spray tip (x < 2 mm), the projected mass evolution is nearly indistinguishable from the one at t = 0.7 ms, then rises rapidly, reaches a maximum value at $x \approx 3.8$ mm and drops sharply to 0. There is no unusual decrease in $M'(x, y_0)$ behind the leading spray edge, which shows that there is no separation between the spray tip and the following droplets in the primary breakup region.

A comparison of $M'(x, y_0)$ and $M'_L(x)$ reveals additional features of the spray tip: the maximum of $M'_L(x)$ is closer to the outlet than the maximum of $M'(x, y_0)$, and the difference between the value at maximum and behind the spray tip is more pronounced for the total than the projected mass. This suggests a wide, mushroom-shaped mass distribution in the spray tip, similar in appearance to corresponding optical images and the two-dimensional projection of Fig. 2a.

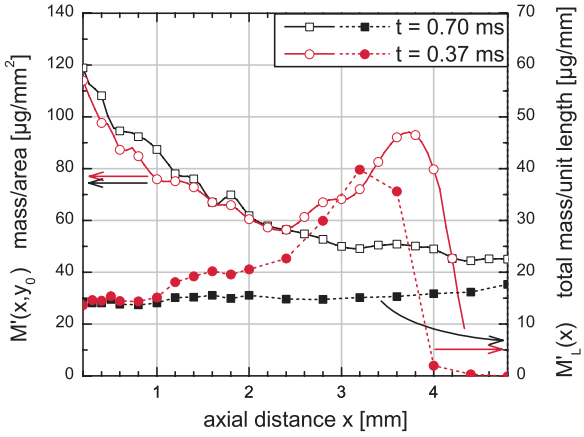

Figure 7: Projected mass $M'(x, y_0)$ in the spray center (calculated dynamically according to Eq. (2); solid curves) and total mass $M'_L(x)$ (dotted curves) as a function of the distance x from the nozzle outlet (ρ_G = 11.4 kg/m^3; the curves are similar at higher ambient density but more difficult to interpret due to a lower signal-noise ratio).

Tentative Reconstruction of the 3-D Spray Structure

Assuming perfect rotational symmetry of the spray, a reconstruction of the (three-dimensional) radial mass distribution can be attempted using the projection slice theorem. Since this method is extremely sensitive to noise, the reconstruction can only work if the data is carefully smoothed prior to these calculations.

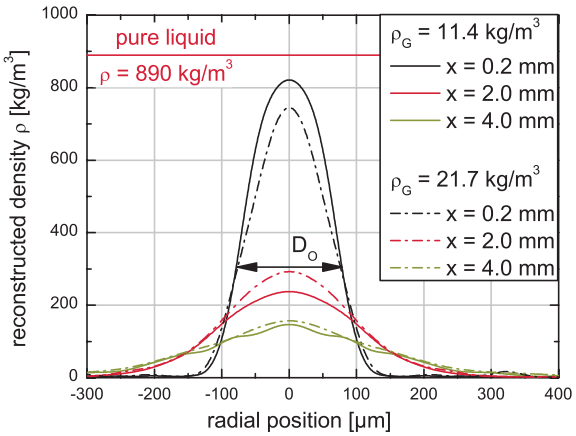

Figure 8: Calculated local density at different distances from the nozzle exit. As the scatter of individual reconstructions is quite large (around ±70 kg/m^3 near the spray axis), average values within a quasi-steady-state time window (t = 0.6-0.8 ms) are shown. The reference density of 890 kg/m^3 is from the fuel/Ce-additive mixture at room temperature.

While it should not be expected a priori that the sprays from multi-hole nozzles have to be symmetric around the spray hole axis, the radial projected mass profiles (Fig. 3) show that the asymmetry is rather small during the quasi-steady-state phase. Figure 8 shows some examples of reconstructed radial mass distributions. Given the restrictions discussed previously, the results should be interpreted only as orders of magnitude. Thus, while the maximum values of the reconstructed densities (at $x = 0.2$ mm) are close to the density of the pure liquid fuel, the question of whether there is an intact liquid core (as has been suggested in [15] and [16]) at the spray center cannot be answered. However, as the maximum value of the reconstructed density decreases very rapidly with increasing x, it becomes apparent that despite the seemingly low values of the spray cone angles, there is a very rapid atomization of the fuel spray. If a quasi-stationary intact liquid core exists, its length must be well below 2 mm, supporting the widely held view that high pressure Diesel sprays are atomized within a few nozzle diameters downstream of the nozzle outlet [2].

Summary

The experiments presented in this paper are a major breakthrough towards the ambitious objective of performing x-ray radiography measurements of Diesel sprays under realistic engine conditions. The densities of the nitrogen atmospheres into which the injections took place were much higher than in all previous measurement campaigns, and, for the first time, a near-standard production nozzle was used. At a given operating point and at two different gas densities, the spray behavior in the near-nozzle region was described in great detail, yielding quantitative data that is not available from any other source. It was found that in very dense atmospheres, the exact value of the gas density has only a small influence on the mass distribution in the Diesel jets, which were generally stable and symmetric. Even though the bulk of the fuel mass is concentrated in a narrow region around the nozzle axis, there is clear evidence for a rapid mixing of gas and liquid.

The current understanding of Diesel sprays is mostly based on results obtained from experiments where single hole axial nozzles were used. Therefore, measurement campaigns similar to the one presented here, but at different operating points or with different injection equipment should be very valuable both to the spray research and to the engine development communities. However, due to the inevitable fog formation inside spray chambers and droplet deposition onto their windows, and because of the significant x-ray extinction of dense gases, such experiments are much more challenging than investigations concentrating on sprays emerging from single hole nozzles under atmospheric conditions. Thus, it may not be straightforward to expand the measurement zone beyond the primary breakup region or to use nozzles with more than three spray holes.

References

[1] G. Bittlinger et al., Die Einspritzdüsenkonfiguration als Mittel zur gezielten Beeinflussung der motorischen Gemischbildung und Verbrennung, *Proc. 6th Congress on Engine Combustion Processes and Modern Techniques*, pp. 19-30, 2003

[2] G. Smallwood and Ö. Gülder, Views on the Structure of Transient Diesel Sprays, *Atomization and Sprays*, 10:355-386, 2000

[3] A.G. MacPhee et al., X-Ray Imaging of Shock Waves Generated by High-Pressure Fuel Sprays, *Science*, 295:1261-1263, 2002

[4] C.F. Powell et al., Effects of Ambient Pressure on Fuel Sprays as Measured Using X-Ray Absorption, *Proc. 16th ILASS Americas*, Monterey, CA, 2003

[5] S. Ciatti et al., Comparison of X-Ray Based Fuel Spray Measurements with Computer Simulation Using the CAB Model, *Proc. CIMAC Congress*, Paper 264, Tokyo, 2004

[6] A.L. Kastengren et al., Determination of Diesel Spray Axial Velocity Using X-Ray Radiography; *SAE Paper 01-0666*, 2007

[7] L. Araneo, A. Coghe, G. Brunello and G.E. Cossali, Experimental Investigation of Gas Density Effects on Diesel Spray Penetration and Entrainment, *SAE Paper 01-0525*, 1999

[8] J. Walther, Quantitative Untersuchung der Innenströmung in kavitierenden Dieseleinspritzdüsen, *Ph.D. Thesis, TU Darmstadt*, 2002

[9] G. Bittlinger et al., Optische Methoden zur Bewertung der dieselmotorischen Gemischbildung und Verbrennung, *Diesel- und Benzindirekteinspritzung (Proc. 5th Conference, Haus der Technik)*, Berlin, 2006

[10] J. Winter et al., Nozzle Hole Geometry - a Powerful Instrument for Advanced Spray Design, *Proc. THIESEL Conference*, Valencia, 2004

[11] A.K. Cline and R.L. Renka, A Storage-Efficient Method for Construction of a Thiessen Triangulation, *Rocky Mountain Journal of Mathematics*, 14:119-139, 1984

[12] P. Leick, G. Bittlinger and C. Tropea, Velocity Measurements in the Near-Nozzle Region of Common-Rail Diesel Sprays at Elevated Back-Pressures, *Proc. 19th ILASS Europe*, Nottingham, 2004

[13] Robert Bosch GmbH. (ed), Dieselmotor-Management, 4th edition, *Vieweg*, 2004

[14] M. Blessing et al., Analysis of Flow and Cavitation Phenomena in Diesel Injection and its Effects on Spray and Mixture Formation, *SAE Paper 01-1358*, 2003

[15] A. Fath, K.-U. Münch and A. Leipertz, Spray Breakup of Diesel Fuel Close to the Nozzle, *Proc. 12th ILASS Europe*, Lund, 1996

[16] A.J. Yule and D.G. Salters, A Conductivity Probe Technique for Investigating the Breakup of Diesel Sprays, *Atomization and Sprays*, 4:41-63, 1994